Published in final edited form as:
Cell. 2011 September 2; 146(5): 761–771. doi:10.1016/j.cell.2011.07.019.

Adipocyte lineage cells contribute to the skin stem cell niche to drive hair cycling

Eric Festa[1], **Jackie Fretz**[2], **Ryan Berry**[5], **Barbara Schmidt**[5], **Matthew Rodeheffer**[1,3,4], **Mark Horowitz**[2], and **Valerie Horsley**[1,4]

[1]Department of Molecular, Cell and Developmental Biology, Yale University

[2]Department of Orthopædics and Rehabilitation, Yale University

[3]Section of Comparative Medicine, Yale University

[4]Yale Stem Cell Center, Yale University

[5]Molecular Cell Biology, Genetics and Development Program, Yale University

Keywords

Adipocytes; stem cells; PDGF; skin; hair

Introduction

Tissue niches are essential for controlling stem cell self-renewal and differentiation (Voog and Jones, 2010). Epithelial lineages in the skin are maintained by stem cells that exist in multiple tissue microenvironments (Blanpain and Fuchs, 2006). In particular, the niche for hair follicle stem cells, which reside within the bulge region of the hair follicle, promotes continual and repetitive regeneration of the follicle during the hair cycle. Specialized mesenchymal cells, the dermal papillae (DP), that are associated with the hair follicle can specify epithelial identity, and are thought to control follicular stem cell activity by releasing signaling molecules (Blanpain and Fuchs, 2006; Greco et al., 2009; Rendl et al., 2005). Extrinsic signals, such as bone morphogenetic proteins (BMPs), fibroblast growth factors (FGFs), platelet derived growth factors (PDGFs) and Wnts can activate stem cell activity in the hair follicle (Blanpain and Fuchs, 2006; Greco et al., 2009; Karlsson et al., 1999). Yet, it remains unclear which cells establish the skin stem cell niche.

Multiple changes within the skin occur during the hair follicle's regenerative cycle (Blanpain and Fuchs, 2006). Following hair follicle morphogenesis (growth phase, anagen), the active portion of the follicle regresses (death phase, catagen), leaving the bulge region with a small hair germ that remains dormant during the resting phase (telogen) (Greco et al., 2009). Anagen induction in the next hair cycle is associated with bulge cell migration and proliferation in the hair germ to generate the highly proliferative cells at the base of the

[1]Correspondence should be addressed to Valerie Horsley, valerie.horsley@yale.edu, Dept. of Molecular, Cellular and Developmental Biology, Yale University, 219 Prospect St., Box 208103, New Haven, CT 06520, Tel #203-436-9126, Fax #203-432-6161.

follicle (Greco et al., 2009; Zhang et al., 2009). The activated stem cells then differentiate to form the inner root sheath and hair shaft for the new hair follicle.

During activation of hair growth, the expansion of the intradermal adipocyte layer in the skin doubles the skin's thickness (Butcher, 1934; Chase et al., 1953; Hansen et al., 1984). The growth of the intradermal adipose depot could occur through adipocyte hypertrophy or adipogenesis. While adipocyte hypertrophy involves lipogenesis, adipogenesis requires the proliferation and specification of adipocyte precursor cells into preadipocytes, which exit from the cell cycle and differentiate into mature, lipid-laden adipocytes (Rodeheffer et al., 2008; Rosen and Spiegelman, 2000). Adipogenesis requires the upregulation and transcriptional activity of the nuclear receptor, PPARγ in preadipoctyes (Rosen and Spiegelman, 2000), which can be blocked by specific antagonists, bisphenol A diglycidyl ether (BADGE) and GW9662 (Bendixen et al., 2001; Wright et al., 2000). Whether intradermal adipocytes undergo hypertrophy and/or adipogenesis during the hair cycle is unknown.

Recent data shows that during the hair cycle, mature intradermal adipocytes express *BMP2* mRNA (Plikus et al., 2008), an inhibitory signal for bulge cell activity (Blanpain and Fuchs, 2006; Plikus et al., 2008). In addition, reduced intradermal adipose tissue in transgenic mice overexpressing human apolipoprotein C-I in the skin (Jong et al., 1998), fatty acid transport protein (*FATP*)-4-deficient mice (Herrmann et al., 2003), and $Dgat1^{-/-}$ or $Dgat2^{-/-}$ mice (Chen et al., 2002; Stone et al., 2004) results in abnormalities in skin structure and function such as hair loss, epidermal hyperplasia, and abnormal sebaceous gland function. While these data suggest a regulatory role for adipocytes in the skin, these mutations affect multiple cell types in the skin. Thus, the precise role of intradermal adipocytes in skin biology remains unclear.

In this study, we analyze the role of intradermal adipocytes on follicular stem cell activity. Using histological and functional analysis of cell populations of the adipocyte lineage in the skin, we identify a dynamic process of adipogenesis that parallels the activation of hair follicle stem cells. Functional analysis of adipocyte lineage cells in mice with defects in adipogenesis and in transplantation experiments revealed that immature adipocyte cells are necessary and sufficient to drive follicular stem cell activation. Finally, we implicate PDGF signals produced by immature intradermal adipocyte lineage cells in controlling hair regeneration. These data define active roles for intradermal adipocytes in the regulation of the skin tissue microenvironment.

Results

De novo adipogenesis parallels follicular stem cell activity

To determine whether changes in individual adipocyte cell size contributes to growth of the intradermal adipocyte layer during the hair cycle (Butcher, 1934; Chase et al., 1953; Hansen et al., 1984)(Figures S1A and S1B), we analyzed individual adipocytes during the hair follicle cycle by immunostaining skin sections with antibodies against caveolin 1A, which is enriched on the cell surface of mature adipocytes (Le Lay et al., 2010) and a fluorescent neutral lipid dye, Lipidtox. Morphometric analyses of individual caveolin^{+}, Lipidtox^{+} cells quantified the cross-sectional area (XSA) of intradermal adipocytes. Adipocytes progressively increased in size following morphogenesis of the hair follicle (P4–P15) (Figures 1A and S1C). Following catagen, intradermal adipocyte XSA decreased to the area of adipocytes during morphogenesis. Thus, intradermal adipose tissue growth during follicle maturation occurs at least in part by hypertrophy of mature adipocytes.

To determine whether anagen induction is associated with changes in intradermal adipocytes, we analyzed intradermal adipose tissue during the 2nd hair cycle when anagen activation is slower than the first hair cycle. At P49 when the follicles are in the second telogen, small intradermal adipocytes exist below the dermis distant from the follicles (Figure 1B). At P56, activation of follicular stem cells is initiated in some follicles, as indicated by an enlarged hair germ. The activated follicles are in close proximity to small caveolin$^+$, Lipidtox$^+$ cells that extend from adipose layer toward the growing hair follicle (Figure 1B), suggesting that follicular stem cell activation is associated with changes in the intradermal adipocytes.

To analyze if *de novo* formation of intradermal adipocytes occurs through a proliferative precursor cell during the hair cycle, we determined if proliferative cells expressing perilipin, which is specifically expressed on mature adipocytes (Greenberg et al., 1991), exist in the skin during the hair cycle by pulsing mice for 3 days with BrdU during different stages of the hair cycle (Figure 1C). When mice were pulsed with BrdU before the first telogen (P18–21), no BrdU positive nuclei were detected within perilipin$^+$ adipocytes. In contrast, when mice were pulsed with BrdU following anagen induction from P21–P24, BrdU positive nuclei were located within perilipin$^+$ cellular membranes (Figure 1C).

We further analyzed *de novo* adipocyte formation by examining BrdU incorporation within the nuclei of mature adipocytes (Figure 1C), which were enriched from dermal tissue via enzymatic dissociation and differential centrifugation. Microscopic analysis of isolated cells and analysis of the expression of adipocyte specific mRNAs by real time PCR confirmed the enrichment of mature adipocytes using this isolation procedure (Figure S1D). FACS analysis of BrdU staining in isolated nuclei from mature adipocytes revealed that when 3-day BrdU pulses were performed during the initiation of anagen, 10% of mature adipocyte nuclei exhibited BrdU localization. In contrast, less than 2% of BrdU$^+$ nuclei were detected when mice were pulsed before anagen induction (Figure 1C). Taken together, these data demonstrate that intradermal adipocytes regenerate through a proliferative precursor during anagen induction.

Adipocyte precursor cells are activated during the hair cycle

Adipocyte precursor cells were recently identified in visceral and subcutaneous adipose tissue depots (Rodeheffer et al., 2008)(Figure S2A). To determine if adipocyte precursor cells exist in the skin, we isolated stromal vascular fraction (SVF) cells from the skin dermis at P21, when anagen is induced during the 1st hair cycle. Similar to visceral adipose tissue, adipocyte precursor cells (Lin-, CD34$^+$, CD29$^+$, Sca1$^+$) are present within skin tissue (Figures 2A and S2A). To confirm skin-derived adipocyte precursor cells are functional, we cultured FACS-purified adipocyte precursor cells from the skin. After 3 days of culture, skin-derived adipocyte precursor cells form robust adipocytes, as seen by Oil Red O staining (Figure S2B). In addition, adipocyte precursor cells were able to form caveolin$^+$, Lipidtox$^+$ cells when injected into the intradermal muscle layer of syngeneic mice (Figure S2B). Thus, functional adipocyte precursor cells reside in the skin.

To analyze the number and proliferation of adipocyte precursor cells during the hair cycle, we pulsed mice with BrdU for 3 days during catagen (P15–P18), anagen initiation (P19–P22) or mature anagen (P22–P25), and analyzed the percentage of adipocyte precursor cells. Few adipocyte precursor cells exist in the skin during catagen (Figures 2B and 2C). In contrast, the percentage of adipocyte precursor cells in the CD34$^+$ SVF cell population increased ~four-fold during anagen induction (Figures 2B and 2C) and returned to baseline during maturation of the hair follicle at P25. Therefore, adipocyte precursor cell number peaks in the skin during follicular stem cell activation.

Analysis of BrdU incorporation within adipocyte precursor cells revealed that prior to anagen ~50% of adipocyte precursor cells are proliferating. However, once anagen was initiated, the percentage of proliferative adipogenic cells was reduced to ~25% (Figure 2C). Thus, adipocyte precursor cells are stimulated to proliferate during late catagen to generate an increased population of adipogenic cells during anagen induction. These data correlate with the timing of *de novo* adipocyte generation after anagen induction (Figure 1C).

To further characterize adipocyte precursor cells in the skin, we analyzed the mRNA expression of the adipogenic transcription factor, *PPARγ*. We find that when compared to expression within SVF cells, *PPARγ* is enriched in adipocyte precursors and expressed at ~25% of the mRNA levels of mature intradermal adipocytes (Figure 2D). These data confirm the adipogenic nature of resident intradermal adipocyte precursor cells.

Mouse models alter distinct adipocyte lineage cells in the skin

To define the function of intradermal adipocyte lineage cells during hair follicle regeneration, we analyzed mouse skin prior to and during hair regeneration at P21 in two separate mouse models with genetic mutations that affect adipogenesis (Figure S3A), or of wild-type mice after pharmacological treatments that affect adipocyte lineage cells (Figure S5).

In one genetic model, mice lacking *Early B cell factor 1* (*Ebf1*$^{-/-}$) display a decrease in postnatal intradermal adipose tissue (Hesslein et al., 2009) (Figure S3A). Analysis of *Ebf1* mRNA expression using *in situ* hybridization revealed that *Ebf1* is expressed in the DP in mature, growing hair follicles at P4 (Rendl et al., 2005); however, bulge, hair germ, and DP cells lack *Ebf1* expression during the initiation of a new anagen during the hair cycle (Figure S3B), when adipogenesis is active. This expression pattern was confirmed by real time PCR on isolated DP cells and epithelial cells (Figure S3C).

In another genetic model, the lipoatrophic ‘fatless’ Azip/F1 mouse, mature white adipocytes are lacking throughout the animal, including the skin (Figure S3A), due to the expression of a flag-epitope tagged, dominant-negative form of C/EBP under the control of the aP2 promoter, which normally drives expression of Fatty Acid Binding Protein-4 (FABP4) late in adipogenesis (Moitra et al., 1998). Immunostaining for the Flag epitope expressed within the Azip transgene detected expression of Flag^{+} cells within the immature subcutaneous adipose depot below the skin of Azip mice but not within the skin epithelium of Azip mice (Figure S3D). The lack of Flag^{+} cells in the intradermal adipose depot of Azip skin suggests that aborted mature adipocytes do not persist in the skin of Azip mice.

While both Azip and *Ebf1*$^{-/-}$ mice displayed delayed hair coat formation (to be reported elsewhere), these defects are absent after P15, and catagen proceeded normally in both Azip and *Ebf1*$^{-/-}$ mice (Figure S4A). Both Azip and *Ebf1* null mice display normal epidermal and sebaceous gland proliferation at P21 (Figure S4B) and sebaceous gland size in Azip and *Ebf1*$^{-/-}$ skin was similar to WT at P21 (Figure S4C). Furthermore, Azip and *Ebf1*$^{-/-}$ mice displayed normal DP morphology and T cell numbers (Figures S4D and S4E). These data suggest that these mutant mice do not display any overt changes of non-adipocyte lineage cells within the skin prior to P21.

We next examined the adipocyte lineage in these mutant mice. Using FACS, we find that adipocyte precursors are absent in *Ebf1*$^{-/-}$ skin but slightly elevated in Azip skin (Figure 3A). To analyze adipocyte precursor activity in Azip and *Ebf1* null mice, we defined proliferation within the intradermal adipocytes following 3 days of BrdU injections after P21 (Figure 3B). Due to the lack of mature adipocytes in Azip skin, we analyzed putative adipocytes in the dermis based on their elevated expression of caveolin 1A. Both WT and

Azip mice displayed BrdU$^+$, caveolin$^+$ cells surrounding hair follicles (Figure 3B). However, *Ebf1* null mice lacked proliferative, caveolin$^+$ cells within the dermis. Similarly, the dermis of WT and Azip mice was filled with PPARγ cells, while the dermis of *Ebf1*$^{-/-}$ mice exhibited few PPARγ cells (Figure 3C). These data suggest that adipocyte precursor cells are able to proliferate and differentiate into highly expressing PPARγ$^+$ preadipocytes in the dermis of WT and Azip mice, but these early adipogenic events are absent within the skin of *Ebf1*$^{-/-}$ mice.

In addition to these genetic models that diminish adiposity in the skin, we treated mice with PPARγ antagonists, bisphenol A diglycidyl ether (BADGE) and GW9662 (Bendixen et al., 2001; Wright et al., 2000) to inhibit adipogenesis pharmacologically (Figure 4). Based on the lack of a phenotype in mice lacking PPARγ in the skin epithelium prior to 3 months of age (Karnik et al., 2009; Mao-Qiang et al., 2004), we did not anticipate dramatic alterations in the function of epithelial cells with the short use of these drugs in 3-week old mice.

To determine if treatment with PPARγ antagonists altered the regeneration of intradermal adipose tissue during anagen activation, we treated mice with BADGE and GW9662 from P18-P24. BADGE- and GW9662-treated skin exhibited a reduction in skin adipose thickness (Figure S5A). To determine if intradermal adipocyte precursor cell number was altered with treatment of PPARγ antagonists, we quantified the percentage of adipocyte precursor cells in vehicle, BADGE- and GW9662-treated mice compared to SVF. In mice treated with BADGE and GW9662 from P18–P24, the percentage of adipogenic cells at P24 was elevated compared to the vehicle-treated mice (Figure 4A). Furthermore, intradermal PPARγ expression was decreased in BADGE- and GW9662-treated mice compared to vehicle (Figure 4B). Interestingly, if treatment of BADGE was delayed until after intiation of anagen at P21 (P21–P27), intradermal adipose tissue displayed normal intradermal adipose tissue size and PPARγ expression (Figures 4B and 4C). These results demonstrate that inhibition of PPARγ prior to anagen induction blocks intradermal adipose tissue regrowth by blocking the action of adipocyte preadipocytes but not reducing the number of adipocyte precursor cells.

To confirm that BADGE or GW9662 treatment does not alter the homeostasis of sebocytes, which express PPARγ and when aberrant, can alter bulge activity and epidermal homeostasis (Horsley et al., 2006; Karnik et al., 2009; Sundberg et al., 2000), we analyzed Ki67 localization and Lipidtox staining in sebaceous glands of BADGE- or GW9662-treated mice. Treatment of mice with PPARγ antagonists from P18–P24 did not alter the proliferation of cells within the sebaceous gland (Figure S5B) or the size of sebaceous glands (Figure S5C). These results confirm that sebaceous gland homeostasis is not dramatically altered during the short-term loss of PPARγ function in the skin. Additional analysis of Ki67 staining in the epidermis revealed that these PPARγ antagonists did not alter epidermal proliferation (Figure S5B).

Thus, these three mouse models with diminished or absent intradermal adipocytes affect different stages of adipogenesis in the skin. The *Ebf1* null mouse lacks adipocyte precursor cells suggesting that this mutation acts at the adipocyte precursor cell to block postnatal intradermal adipogenesis. PPARγ antagonists do not block the formation of adipocyte precursor cells in the skin but disrupt the formation of PPARγ$^+$, preadipocytes, resulting in a loss of postnatal intradermal adipogenesis. Finally, the Azip transgene blocks late stages of adipocyte maturation after PPARγ$^+$, preadipocyte formation, allowing us to examine the role of mature, lipid-laden adipocytes in the skin.

Adipogenesis defects result in aberrant follicular stem cell activation

Next, we examined the telogen to anagen transition after P19 in WT, Azip, *Ebf1* null and mice treated with PPARγ antagonists. Follicles of *Ebf1* null mice display telogen or late catagen morphology from P21–P56, suggesting that *Ebf1*$^{-/-}$ mice have defects in activation of bulge stem cells (Figure 3D). These defects were evident morphologically and by the lack of BrdU incorporation in hair germ cells after a 24 hr pulse (Figure S3E). In contrast, Azip mice displayed anagen induction kinetics similar to WT mice (Figure 3D), as evidenced by anagen morphology and proliferation within the hair germ in the majority of Azip follicles at P21 (Figure S3E). Taken together, these data suggest that immature adipocyte lineage cells, which are absent in *Ebf1*$^{-/-}$ mice but present in Azip mice, are necessary for follicular stem cell activation.

Since *Ebf1*$^{-/-}$ mice may display defects in the skin based on *Ebf1* expression in the DP at P4, we determined if the lack of adipocyte lineage cells are the primary defect that results in hair cycling defects in *Ebf1*$^{-/-}$ mice using skin grafting experiments. Skin was isolated from P18 female WT or *Ebf1*$^{-/-}$ mice, scraped to remove intradermal adipocytes, and grafted onto full thickness wounds of male *Ebf1*$^{-/-}$ or WT littermates, respectively. Three weeks after grafting, hair growth was evident in the grafts from *Ebf1*$^{-/-}$ mice on WT recipients, whereas WT grafts lacked external hair follicles when grafted onto male *Ebf1*$^{-/-}$ mice (Figure S3F). We verified that dermal cells in these grafts were derived from the male recipients using *in situ* hybridization for the Y chromosome (Figure S3F). Importantly, the epithelium and DP in anagen follicles were derived from the female *Ebf1*$^{-/-}$ donor skin, suggesting that inherent defects in hair follicle cells of *Ebf1*$^{-/-}$ mice do not prohibit hair growth induction.

To further confirm if adipocyte lineage cells are able to rescue hair cycling defects of *Ebf1*$^{-/-}$ mice, we transplanted WT adipocyte precursor cells, which were FACS isolated from skin total dermal SVF, into *Ebf1*$^{-/-}$ skin at P21. As a control, the contralateral side of the backskin was injected with total WT SVF cells, which consists of unfractionated cells isolated from the dermis. Three days post-injection, follicles within WT SVF-injected *Ebf1*$^{-/-}$ mice remained in telogen as indicated by follicle morphology and by the lack of Ki67^{+} hair germ cells, which indicates anagen at early stages of activation (Figure 5C). In contrast, regions of *Ebf1*$^{-/-}$ backskin injected with WT adipocyte precursor cells displayed Ki67^{+} cells within the hair germ of follicles and were adjacent to Y chromosome^{+} cells when WT male cells were injected into *Ebf1*$^{-/-}$ female recipient mice (Figure 5C). When cell transplantations were followed for 2 weeks, follicles in *Ebf1* null skin injected with WT adipocyte precursor cells were in full anagen, while the SVF injected skin remained in telogen (Figure 5C). Together with the skin grafting experiments (Figure S3F), these data strongly suggest that the lack of adipocyte precursor cells in *Ebf1* null mice at P21 is the likely cause for the lack of follicular stem cell activation in *Ebf1*$^{-/-}$ mice, and the function of Ebf1 in other skin cell types, such as DP cells, is likely not responsible for the hair cycle phenotype.

Next, we examined whether PPARγ^{+} preadipocytes in the skin were necessary to induce follicular regeneration. To do so, we analyzed mice treated with BADGE and GW9662 during the transition from telogen to anagen from P18–P24. As controls, we treated mice with vehicle from P18–P24 or with BADGE from P21–P27 after anagen induction. The hair follicles of both mice treated with vehicle and mice treated with BADGE from P21–P27 generated anagen follicles normally with almost 100% of the follicles in anagen after 6 days of treatment (Figures 4C). In contrast, mice treated with BADGE or GW9662 from P18–P24 did not enter into anagen and remained in the telogen phase of the hair cycle (Figure 4C). These data indicate that preadipocytes with functional PPARγ nuclear receptors are necessary for regeneration of the hair follicle.

Adipocytes are sufficient to induce follicular stem cell activation

To determine if adipocyte lineage cells are sufficient to alter follicular stem cell activity, we intradermally grafted adipocyte precursor cells derived from the SVF of subcutaneous adipose tissue from mice expressing luciferase under the *leptin* promoter (Rodeheffer et al., 2008). We used 6–8 week old mice since murine hair follicles enter into an extended telogen phase that lasts for 3–4 weeks around 7 weeks of age. When shaved mice were injected with adipocyte precursor cells into the ventral region of WT mice, luciferase activity was identified at the injection site after 6 weeks (Figure 5A). Interestingly, mice with robust adipocyte formation displayed external hair growth in the injected area (Figure 5A).

To further determine if the hair growth-inducing activity of adipocyte lineage cells is enriched compared to unfractionated SVF cells, we injected SVF or FACS-isolated subcutaneous adipocyte precursor cells into the dermis of shaved, murine backskin at 7 weeks of age. Both cell populations were injected into the same region of the backskin to avoid differences in the hair follicle stage due to regional differences in the skin (Plikus et al., 2008). Two weeks following cell engraftment, hair growth was evident at the adipocyte precursor cell injection site but not on the adjacent side injected with SVF cells (Figure 5B). Histological analysis of skin from these mice revealed morphological anagen induction in the adipocyte precursor injected skin but not in the skin injected with SVF cells (Figures 5B). These data suggest that adipocyte lineage cells are sufficient to induce precocious hair follicle regrowth.

To determine if immature adipocyte lineage cells or mature adipocytes are sufficient to induce hair follicle growth, we determined if adipocyte precursor cells derived from Azip mice could induce anagen in syngeneic WT mice at P49. Since mature adipocytes cannot be transplanted by current methods without adipocyte precursor cell engraftment, induction of anagen by Azip adipocyte lineage cells would indicate that mature adipocytes are not the primary adipogenic cell type involved in the induction of stem cell activity in hair follicles. When we injected SVF cells derived from Azip mice, $Flag^+$ cells were absent from the skin and hair follicles remained in telogen (Figure 5D). However, in the areas of skin injected with adipocyte precursor cells from Azip mice, $Flag^+$ cells were evident within the skin and were adjacent to hair follicles entering into anagen, as indicated by the enlarged hair germ morphology and Ki67 staining in the hair germ (Figure 5D). Taken together, these data suggest that immature adipocyte lineage cells initiate hair growth through the activation of follicular stem cell activity.

Defective PDGF signaling in follicles without adipocyte regeneration

To characterize potential molecular mechanisms by which adipocytes regulate hair follicle cycling, we analyzed skin sections in WT and $Ebf1^{-/-}$ mice for activation of signaling pathways that regulate follicular homeostasis and regeneration (Blanpain and Fuchs). Specifically, we immunostained skin sections with antibodies against phospho-SMAD1/5/8, phospho-42/44 MAP kinase, and β-catenin to analyze bone morphogenetic, growth factor, and Wnt signaling, respectively. While nuclear β-catenin and phospho-SMAD1/5/8 were localized to the nuclei of cells within hair follicles in P7 *Ebf1* null mice, as is observed in WT mice, phosphorylation of MAP kinase (p42/44) was diminished in *Ebf1* null follicles compared to WT follicles (Figure 6A). This lack of MAP kinase activation extended to anagen induction, where phospho-$MAPK^+$ nuclei were found in WT follicles in the hair germ and DP, but $Ebf1^{-/-}$ follicles lacked phospho-MAPK localization in both of these cell types (Figure 6B).

To define candidate molecules expressed by adipocyte lineage cells that could mediate cell signaling, we analyzed mRNA expression for molecules that have been implicated in hair

follicle cycling in skin-derived adipocyte precursor cells and mature adipocytes. As described previously, BMP expression is enriched in mature adipocytes (Plikus et al., 2008) (Figure 6C). Interestingly, the expression of PDGFA in adipocyte precursor cells was elevated almost 100 fold over the expression in SVF cells. Mice lacking *PDGFA* display phenotypic similarities with *Ebf1* null mice, including a delay of follicle stem cell activation that blocks anagen induction (Karlsson et al., 1999; Tomita et al., 2006).

To determine if mice with defects in intradermal adipocyte regeneration display defective PDGF signaling, we analyzed the expression and activity of the PDGF receptor (PDGFR) by immunofluorescence in WT, *Ebf1*$^{-/-}$ and BADGE-treated skin. We find that during telogen and anagen, PDGFR is expressed below the bulge in the DP as described previously (Rendl et al., 2005) (Figure 6D). Analysis of phospho-PDGFR demonstrated that during anagen induction, PDGFR is activated in the DP and the lower part of the hair germ (Figure 6E). To determine if intradermal adipose regeneration is required for activation of the PDGFR, we analyzed hair follicles from BADGE-treated and *Ebf1* null mice for activation of the PDGFR at P21. As seen in Figure 6E, PDGFR activation was diminished in the DP of both BADGE-treated and *Ebf1* null mice.

Based on the data above, we hypothesized that PDGF signaling may be defective in *Ebf1* null mice, which lack adipocyte precursor cells. Thus, we tested whether elevated PDGFA could trigger the activation of stalled hair follicle regeneration in *Ebf1* null mice. To this end, we injected PDGFA-coated beads intradermally into *Ebf1* null mice at P21. Three days after bead implantation, a majority of follicles adjacent to PDGFA-coated beads displayed morphologies characteristic of anagen follicles (Figures 6F). This growth induction increased with elevated concentrations of PDGFA with 100ng/μl activating ~86% of adjacent follicles, demonstrating a dose dependency of activation of *Ebf1* null hair follicles. By contrast, follicles in *Ebf1* null mice that were adjacent to BSA-coated beads remained in telogen. Taken together, these data suggest that intradermal adipocyte precursor cells activate PDGF signaling in the DP in a dynamic manner.

Discussion

Our data support a model in which cells of the adipocyte lineage form a niche within mammalian skin to regulate epithelial stem cell behavior (Figure 7). Using mouse models with defects in adipose tissue, we probed the role of immature and mature adipocytes in the skin. The relatively normal activation of hair follicle growth in Azip mice, which lack mature adipocytes, when taken together with the lack of follicular stem cell activation in *Ebf1* null and PPARγ antagonist treated mice, which have defects in immature adipocytes, support an active role of immature adipocytes during the activation of hair growth. Future experiments analyzing the role of mature adipocytes in hair cycling and skin homeostasis may reveal their function in the skin, as suggested by the expression of *BMP* mRNA in these cells (Figure 6)(Plikus et al., 2008).

Adipocyte lineage cells in other tissues have been shown to generate niches for other cell types. Hematopoietic stem cell engraftment is inhibited by mature adipocytes within bone marrow (Naveiras et al., 2009). In contrast, mature adipocytes positively regulate the formation of the mammary gland epithelium for efficient branching and development (Couldrey et al., 2002; Landskroner-Eiger et al., 2010). In addition, adipocyte precursor cells have also been found within skeletal muscle and may signal to muscle precursor cells to promote muscle differentiation (Joe et al., 2010; Uezumi et al., 2010). Combined with our data showing that adipocyte precursor cells are necessary and sufficient for the activation of skin epithelial stem cells, these studies highlight the importance of cells in the adipocyte lineage as niche cells within individual tissues.

Based on the expression of *PDGF* ligands by adipocyte lineage cells, the activation of the PDGFR in the DP during anagen, and the ability of PDGF-coated beads to rescue hair cycling defects in *Ebf1* null mice, we propose that adipocyte precursor cells secrete PDGF to promote hair growth. Mice lacking PDGF-A display similar hair follicle defects as *Ebf1* null mice, namely a lack of anagen entry (Karlsson et al., 1999). In addition, PDGF ligands have been implicated in hair growth induction based on experiments analyzing conditioned media from SVF derived adipocytes (Park et al., 2010). Adipocyte lineage cells are not the only cell type in the skin that expresses PDGF ligands, multiple cells in the follicular epithelium, the matrix and the hair germ, have been shown to express PDGF (Karlsson et al., 1999). Additional signals expressed by intradermal adipocytes may also be involved in signaling to the DP or epithelium (Park et al., 2010). Future experiments will clarify the cellular target of adipocyte signals in the skin and further define how PDGF signaling promotes bulge cell activation.

Our data also suggest that the intradermal adipose tissue is regulated in a manner that is distinct from other adipose depots. In general, the turnover of adipose in subcutaneous and visceral fat is relatively slow (Ochi et al., 1988; Spalding et al., 2008). However, we find dramatic alterations in intradermal adipose tissue that parallels the rapid turnover of the hair follicle. Identification of mechanisms that regulate intradermal adipose tissue dynamics may have relevance for the growth and atrophy of other adipose depots. While the origin of precursor cells within adipose tissue *in vivo* is not well understood, a population of cells within the skin (skin-derived precursors (SKPs)) was suggested to repopulate multiple cell lineages within the dermis, including adipocytes (Biernaskie et al., 2009). Defining the relationship between intradermal adipocyte turnover, SKPs, and other dermal populations in the skin may reveal novel mechanisms involved in turnover of the intradermal adipocytes.

It is interesting to note that human patients with obesity, anorexia, and lipodystrophy have hair follicle growth defects (Fukumoto et al., 2009; Lurie et al., 1996; Piacquadio et al., 1994). By defining the role of the understudied adipocyte lineage cells in the skin, we have identified that these cells dynamically promote epithelial stem cell activity. Whether cells of the adipocyte lineage also play a role in other processes in the skin, such as tumorigenesis and wound healing, is not known. It will be important for future studies to determine whether adipocytes can act during these clinically relevant pathological conditions.

Experimental Procedures

Mice and treatments with BrdU and PPARγ antagonists

Azip and *Ebf1* null mice have been described previously (Lin and Grosschedl, 1995; Moitra et al., 1998). For 5-Bromo-2’-deoxyuridine (BrdU) pulse experiments, mice were injected intraperitoneally with 50 μg/g BrdU (Sigma-Aldrich) prior to being sacrificed. For experiments using PPARγ antagonists, mice were treated daily with BADGE at 15μg/g or GW9662 at 1μg/g. All animals were handled according to the Institutional guidelines of Yale University.

Histology and Immunofluorescence

Skin was mounted using O.C.T. compound, sectioned, fixed in a 4% formaldehyde solution. When applicable the M.O.M. kit (Vector labs) was used to prevent non-specific binding with mouse antibodies. Antibodies and their dilutions are listed in Supplemental Methods. Fluorescence staining of lipids was performed using Lipidtox (1:200, Invitrogen). For histological analysis, the sections were stained with hematoxylin and eosin. Alkaline Phosphatase staining was performed using Western Blue Stabilized Substrate according to manufacturer’s instructions (Promega).

Flow cytometry analysis and sorting

SVF cells were released from the dermis of skin tissue via digestion of minced tissue with collagenase IA (Sigma). Adipocyte precursor cell purification was performed as described (Rodeheffer et al., 2008). Briefly, single cell suspensions were resuspended in FACS staining buffer containing PBS and 4% fetal bovine serum and stained with antibodies described in Supplemental methods. Cells were sorted using FACS Aria equipped with FACS DiVA software (BD Biosciences).

Isolation of mature adipocytes was performed following collagenase digestion as described above. Released SVF cells were centrifuged, floating cells isolated and washed in adipocyte wash buffer containing Hank's buffered saline solution (HBSS) with 3% bovine serum albumin (BSA) solution. Following resuspension in adipocyte wash buffer, the cells were then lysed by addition of 0.2% NP40. The nuclei were pelleted via centrifugation and stored in wash buffer containing 0.02% NP40. BrdU staining of cells and mature adipocyte nuclei was performed according to manufacturer's directions using the Brdu Flow kit (BD Biosciences).

Adipocyte culture

Freshly isolated skin-derived SVF cells or purified adipocyte precursor cells were plated onto laminin-coated plates (BD Biosciences) in DMEM supplemented with 10% FBS (GIBCO) and 10 ng/mL bFGF (R&D Systems) and maintained in a 5% CO2 atmosphere. Cells were allowed to grow to confluence and were then held at confluence for 3 days without bFGF. For staining, cells were fixed with 2% formaldehyde and 0.2% glutaraldehyde in PBS for 15 min and then rinsed in PBS, water, and 60% isopropanol sequentially. The cells were then stained with Oil red O (0.7% in 60% isopropanol).

Skin grafts, cell transplantations and bead injections

For skin grafts, donor skin from P18 female mice was dissected, scraped to remove intradermal adipocytes, and grafted onto full thickness wounds of male littermate mice. Skins were prepared for histological analysis after the appearance of hair growth at D21. Intradermal cell transplantations were performed with 5×10^5 SVF cells or FACS purified adipocyte precursor cells. Three days to 2 weeks following injection, skins were prepared for histological analysis. Cell and tissue grafting was performed at least twice in at least 2 mice per experiment.

For injection of PDGF beads intradermally, recombinant human PDGF (R&D Systems) was reconstituted in 0.1% BSA. Affi-gel blue beads (Bio-Rad) were washed in PBS, incubated in protein solution at 37°C for 30 min. As a control, beads were incubated in 0.1% BSA alone. For the dosage analysis, 1ng/μl, 10ng/μl, 100ng/μl of PDGF were used to coat beads. Approximately 15–20 coated beads were injected into the skin of *Ebf1* null mice. Skins were harvested 3 days after injections to determine activation status of hair follicles.

In situ hybridization and probes

Antisense cRNA probes directed against mouse *Ebf1* (GenBank accession # NM_007897, 1195–2248 bp) (Jin et al., 2010) were generated following the manufacturer's protocol (Roche). Cryosections of mouse skin were fixed with 4% formaldehyde, washed with PBS and acetylated in 0.1M triethanolamine HCl, pH 8.0, 233mM NaOH, and 0.25% acetic anhydride. Sections were then hybridized with cDNA probes in 50% hybridization buffer (TBS with 5% heat-inactivated sheep serum, 50% formamide) overnight at 55°C. Sections were washed with SSC and Wash Buffer (Roche) and probe detection was performed according to manufacturer's instructions (Roche). Y chromosome *in situ* hybridization was performed on frozen skin sections according to manufacturer's protocol (IDetect

Chromosome Paint Mouse Probe, ID Labs). Sections were hybridized with cDNA probes at 37°C for 5 hours. For both *in situ* hybridization protocols, sections were mounted in Prolong Gold with DAPI (Invitrogen) and subjected to brightfield and fluorescent microscopy.

Statistics

To determine significance between groups, comparisons were made using Students t tests. Analyses of multiple groups were performed using One-Way ANOVA with Bonferroni's posttest with GraphPad Prism version for Macintosh (GraphPad Software). For all statistical tests, the 0.05 level of confidence was accepted for statistical significance.

Supplementary Material

Refer to Web version on PubMed Central for supplementary material.

Acknowledgments

We thank Dr. Mengqing Xiang for the vector encoding the *Ebf1* in situ hybridization probe and Drs. Ana Tadeu and Natalie Roberts for assistance with experiments. Horsley lab members and Drs. Michael Rendl and Tudorita Tumbar provided critical reading of the manuscript and valuable discussions. V.H. is a Pew Scholar in Biomedical Research and is funded by the NIH (4R00AR054775) and the Connecticut Dept. Public Health (09SCAYALE30). M.H. is funded by AR052690, AR046032 and DK084970 from NIH (NIDDK and NIAMS). M.R. is supported by 5P30DK045735-18 from NIDDK/NIH.

Bibliography

Bendixen AC, Shevde NK, Dienger KM, Willson TM, Funk CD, Pike JW. IL-4 inhibits osteoclast formation through a direct action on osteoclast precursors via peroxisome proliferator-activated receptor gamma 1. Proc Natl Acad Sci U S A. 2001; 98:2443–2448. [PubMed: 11226258]

Biernaskie J, Paris M, Morozova O, Fagan B, Marra M, Pevny L, Miller F. SKPs derive from hair follicle precursors and exhibit properties of adult dermal stem cells. Cell Stem Cell. 2009; 5:610–623. [PubMed: 19951689]

Blanpain C, Fuchs E. Epidermal stem cells of the skin. Annu Rev Cell Dev Biol. 2006; 22:339–373. [PubMed: 16824012]

Butcher EO. The hair cycles in the albino rat. (The Anatomical Record), pp. 1934:5–19.

Chase H, Montagna W, Malone J. Changes in the skin in relation to the hair growth cycle. Anat Rec. 1953; 116:75–81. [PubMed: 13050993]

Chen H, Smith S, Tow B, Elias P, Farese RJ. Leptin modulates the effects of acyl CoA:diacylglycerol acyltransferase deficiency on murine fur and sebaceous glands. J Clin Invest. 2002; 109:175–181. [PubMed: 11805129]

Couldrey C, Moitra J, Vinson C, Anver M, Nagashima K, Green J. Adipose tissue: a vital in vivo role in mammary gland development but not differentiation. Dev Dyn. 2002; 223:459–468. [PubMed: 11921335]

Fukumoto D, Kubo Y, Saito M, Arase S. Centrifugal lipodystrophy of the scalp presenting with an arch-form alopecia: a 10-year follow-up observation. J Dermatol. 2009; 36:499–503. [PubMed: 19712277]

Greco V, Chen T, Rendl M, Schober M, Pasolli H, Stokes N, Dela Cruz-Racelis J, Fuchs E. A two-step mechanism for stem cell activation during hair regeneration. Cell Stem Cell. 2009; 4:155–169. [PubMed: 19200804]

Greenberg AS, Egan JJ, Wek SA, Garty NB, Blanchette-Mackie EJ, Londos C. Perilipin, a major hormonally regulated adipocyte-specific phosphoprotein associated with the periphery of lipid storage droplets. J Biol Chem. 1991; 266:11341–11346. [PubMed: 2040638]

Hansen LS, Coggle JE, Wells J, Charles MW. The influence of the hair cycle on the thickness of mouse skin. The Anatomical Record. 1984; 210:569–573. [PubMed: 6524697]

Herrmann T, van der Hoeven F, Grone HJ, Stewart AF, Langbein L, Kaiser I, Liebisch G, Gosch I, Buchkremer F, Drobnik W, et al. Mice with targeted disruption of the fatty acid transport protein 4 (Fatp 4, Slc27a4) gene show features of lethal restrictive dermopathy. J Cell Biol. 2003; 161:1105–1115. [PubMed: 12821645]

Hesslein D, Fretz J, Xi Y, Nelson T, Zhou S, Lorenzo J, Schatz D, Horowitz M. Ebf1-dependent control of the osteoblast and adipocyte lineages. Bone. 2009; 44:537–546. [PubMed: 19130908]

Horsley V, Aliprantis A, Polak L, Glimcher L, Fuchs E. NFATc1 balances quiescence and proliferation of skin stem cells. Cell. 2008; 132:299–310. [PubMed: 18243104]

Horsley V, O'Carroll D, Tooze R, Ohinata Y, Saitou M, Obukhanych T, Nussenzweig M, Tarakhovsky A, Fuchs E. Blimp1 defines a progenitor population that governs cellular input to the sebaceous gland. Cell. 2006; 126:597–609. [PubMed: 16901790]

Jin K, Jiang H, Mo Z, Xiang M. Early B-cell factors are required for specifying multiple retinal cell types and subtypes from postmitotic precursors. J Neurosci. 2010; 30:11902–11916. [PubMed: 20826655]

Joe AW, Yi L, Natarajan A, Le Grand F, So L, Wang J, Rudnicki MA, Rossi FM. Muscle injury activates resident fibro/adipogenic progenitors that facilitate myogenesis. Nat Cell Biol. 2010; 12:153–163. [PubMed: 20081841]

Jong MC, Gijbels MJ, Dahlmans VE, Gorp PJ, Koopman SJ, Ponec M, Hofker MH, Havekes LM. Hyperlipidemia and cutaneous abnormalities in transgenic mice overexpressing human apolipoprotein C1. J Clin Invest. 1998; 101:145–152. [PubMed: 9421476]

Karlsson L, Bondjers C, Betsholtz C. Roles for PDGF-A and sonic hedgehog in development of mesenchymal components of the hair follicle. Development. 1999; 126:2611–2621. [PubMed: 10331973]

Karnik P, Tekeste Z, McCormick TS, Gilliam AC, Price VH, Cooper KD, Mirmirani P. Hair follicle stem cell-specific PPARgamma deletion causes scarring alopecia. J Invest Dermatol. 2009; 129:1243–1257. [PubMed: 19052558]

Landskroner-Eiger S, Park J, Israel D, Pollard J, Scherer P. Morphogenesis of the developing mammary gland: Stage-dependent impact of adipocytes. Dev Biol. 2010

Le Lay S, Briand N, Blouin C, Chateau D, Prado C, Lasnier F, Le Liepvre X, Hajduch E, Dugail I. The lipoatrophic caveolin-1 deficient mouse model reveals autophagy in mature adipocytes. Autophagy. 2010; 6

Lin H, Grosschedl R. Failure of B-cell differentiation in mice lacking the transcription factor EBF. Nature. 1995; 376:263–267. [PubMed: 7542362]

Lurie R, Danziger Y, Kaplan Y, Sulkes J, Abramson E, Mimouni M. Acquired pili torti--a structural hair shaft defect in anorexia nervosa. Cutis. 1996; 57:151–156. [PubMed: 8882012]

Mao-Qiang M, Fowler AJ, Schmuth M, Lau P, Chang S, Brown BE, Moser AH, Michalik L, Desvergne B, Wahli W, et al. Peroxisome-proliferator-activated receptor (PPAR)-gamma activation stimulates keratinocyte differentiation. J Invest Dermatol. 2004; 123:305–312. [PubMed: 15245430]

Moitra J, Mason M, Olive M, Krylov D, Gavrilova O, Marcus-Samuels B, Feigenbaum L, Lee E, Aoyama T, Eckhaus M, et al. Life without white fat: a transgenic mouse. Genes Dev. 1998; 12:3168–3181. [PubMed: 9784492]

Naveiras O, Nardi V, Wenzel P, Hauschka P, Fahey F, Daley G. Bone-marrow adipocytes as negative regulators of the haematopoietic microenvironment. Nature. 2009; 460:259–263. [PubMed: 19516257]

Ochi M, Sawada T, Kusunoki T, Hattori T. Morphology and cell dynamics of adipose tissue in hypothalamic obese mice. Am J Physiol. 1988; 254:R740–R745. [PubMed: 3364603]

Park BS, Kim WS, Choi JS, Kim HK, Won JH, Ohkubo F, Fukuoka H. Hair growth stimulated by conditioned medium of adipose-derived stem cells is enhanced by hypoxia: evidence of increased growth factor secretion. Biomed Res. 2010; 31:27–34. [PubMed: 20203417]

Piacquadio D, Rad F, Spellman M, Hollenbach K. Obesity and female androgenic alopecia: a cause and an effect? J Am Acad Dermatol. 1994; 30:1028–1030. [PubMed: 8188870]

Plikus M, Mayer J, de la Cruz D, Baker R, Maini P, Maxson R, Chuong C. Cyclic dermal BMP signalling regulates stem cell activation during hair regeneration. Nature. 2008; 451:340–344. [PubMed: 18202659]

Rendl M, Lewis L, Fuchs E. Molecular dissection of mesenchymal-epithelial interactions in the hair follicle. PLoS Biol. 2005; 3:e331. [PubMed: 16162033]

Rodeheffer M, Birsoy K, Friedman J. Identification of white adipocyte progenitor cells in vivo. Cell. 2008; 135:240–249. [PubMed: 18835024]

Rosen ED, Spiegelman BM. Molecular regulation of adipogenesis. Annu Rev Cell Dev Biol. 2000; 16:145–171. [PubMed: 11031233]

Spalding K, Arner E, Westermark P, Bernard S, Buchholz B, Bergmann O, Blomqvist L, Hoffstedt J, Näslund E, Britton T, et al. Dynamics of fat cell turnover in humans. Nature. 2008; 453:783–787. [PubMed: 18454136]

Stone S, Myers H, Watkins S, Brown B, Feingold K, Elias P, Farese RJ. Lipopenia and skin barrier abnormalities in DGAT2-deficient mice. J Biol Chem. 2004; 279:11767–11776. [PubMed: 14668353]

Sundberg JP, Boggess D, Sundberg BA, Eilertsen K, Parimoo S, Filippi M, Stenn K. Asebia-2J (Scd1(ab2J)): a new allele and a model for scarring alopecia. Am J Pathol. 2000; 156:2067–2075. [PubMed: 10854228]

Tomita Y, Akiyama M, Shimizu H. PDGF isoforms induce and maintain anagen phase of murine hair follicles. J Dermatol Sci. 2006; 43:105–115. [PubMed: 16725313]

Tsai SY, Clavel C, Kim S, Ang YS, Grisanti L, Lee DF, Kelley K, Rendl M. Oct4 and klf4 reprogram dermal papilla cells into induced pluripotent stem cells. Stem Cells. 2010; 28:221–228. [PubMed: 20014278]

Uezumi A, Fukada S, Yamamoto N, Takeda S, Tsuchida K. Mesenchymal progenitors distinct from satellite cells contribute to ectopic fat cell formation in skeletal muscle. Nat Cell Biol. 2010; 12:143–152. [PubMed: 20081842]

Voog J, Jones D. Stem cells and the niche: a dynamic duo. Cell Stem Cell. 2010; 6:103–115. [PubMed: 20144784]

Wright H, Clish C, Mikami T, Hauser S, Yanagi K, Hiramatsu R, Serhan C, Spiegelman B. A synthetic antagonist for the peroxisome proliferator-activated receptor gamma inhibits adipocyte differentiation. J Biol Chem. 2000; 275:1873–1877. [PubMed: 10636887]

Zhang Y, Cheong J, Ciapurin N, McDermitt D, Tumbar T. Distinct self-renewal and differentiation phases in the niche of infrequently dividing hair follicle stem cells. Cell Stem Cell. 2009; 5:267–278. [PubMed: 19664980]

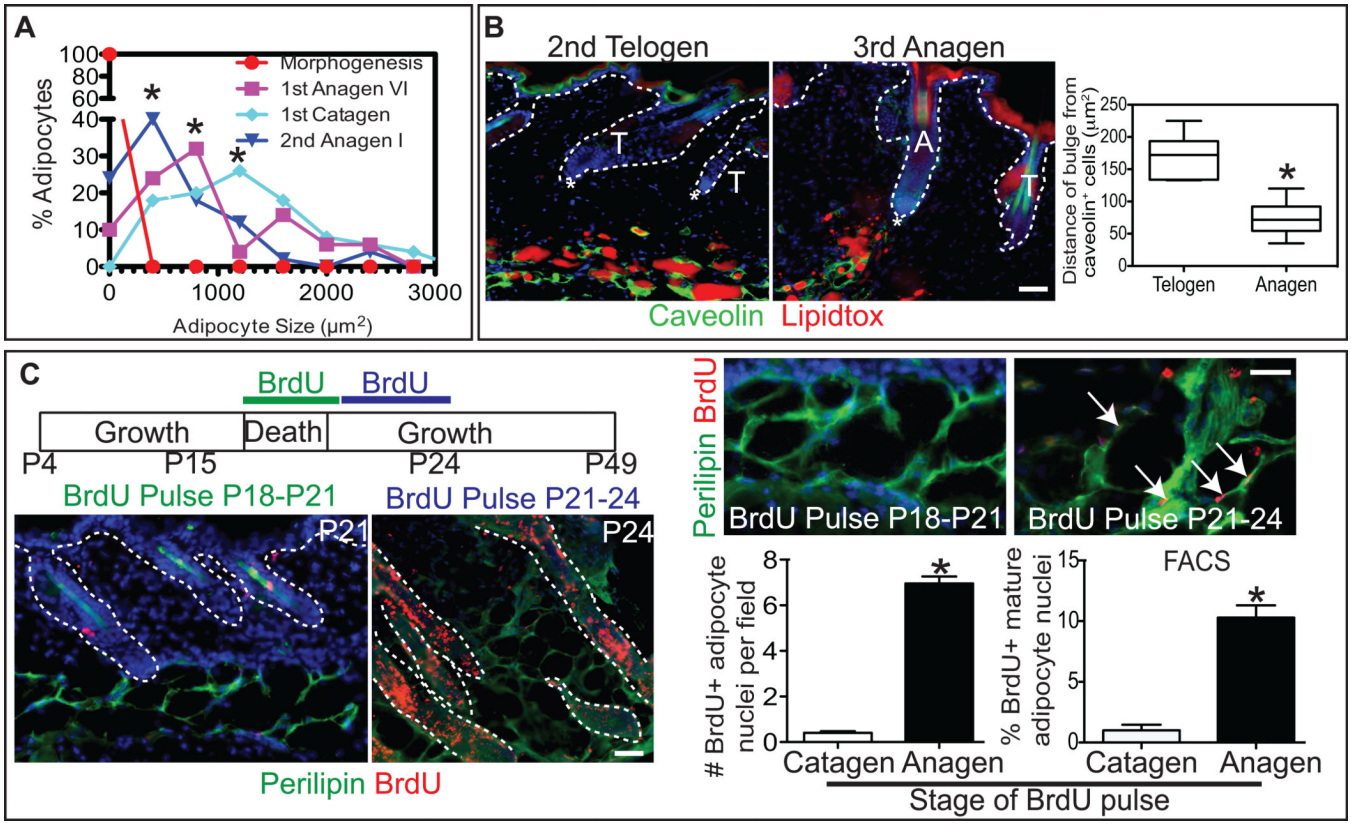

Figure 1. Intradermal adipocytes regenerate via a proliferative precursor cell during the hair cycle

A. Histogram plot of the size distribution of Lipidtox$^+$/caveolin$^+$ cells during the hair cycle. n=80–100 cells from 3–4 mice for each hair cycle stage. Asterisks indicate significance compared to other hair cycle stages. B. Caveolin immunostaining (green) and Lipidtox staining (red) marks intradermal adipocytes during the telogen (P49) and anagen (P56) of the second hair cycle. A, anagen; T, telogen. Dashed lines outline epidermis and hair follicles. Box and whisker plots of the distance of caveolin$^+$ cells from hair follicle bulge at P56. n= 100 follicles from 2 individual mice for each box. C. Schematic of 3-day BrdU labeling experiments during catagen (P18–P21) and anagen (P21–P24). Representative images for perilipin (green), nuclei (blue) and BrdU (red) immunostaining of skin sections. Dashed lines outline epidermis and hair follicles. Arrows indicate perilipin$^+$, BrdU$^+$ cells. Quantification of the number of BrdU$^+$, perlipin$^+$ adipocytes in 20X microscopy fields. n= 3–5 mice; >15 follicles per timepoint. Quantification the % of BrdU$^+$ nuclei of mature adipocytes as analyzed by FACS. n= 3–5 mice for each bar. All data are ± SEM, *p<0.05. Bars=100μm. See also Figure S1.

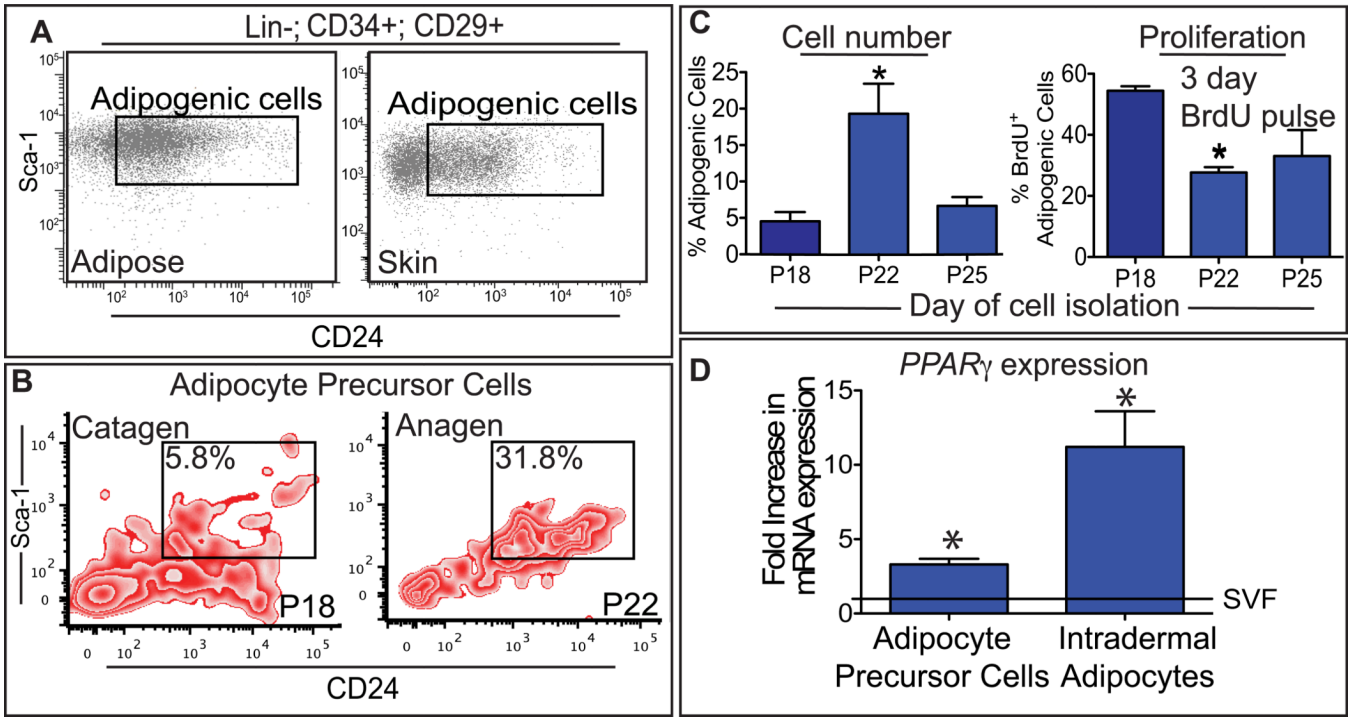

Figure 2. Resident skin adipocyte precursor cells display dynamic activity associated with the hair cycle

A. Representative FACS plots of Sca1^{+}, CD24$^{+/-}$ adipogenic cells within the CD31/CD45 negative (Lin-), CD34^{+}, and CD29^{+} gated cell populations in subcutaneous adipose tissue or P21 skin. B. Representative FACS plots of adipocyte precursor cells from skin in catagen (P18) or early anagen (P22). C. Graphs quantify the % of adipogenic cells and the % of BrdU^{+} adipogenic cells within the Lin^{-}, CD29^{+}, and CD34^{+} cell population at P18 (catagen), P22 (initial anagen) or P25 (mid-anagen). D. Real-Time PCR analysis of *PPARγ* mRNA expression in P21 adipogenic cells and mature intradermal adipocytes compared to total isolated stromal vascular fraction (SVF) in the skin. n=3 independently isolated cell populations. All data are ± SEM, *p<0.05. See also Figure S2.

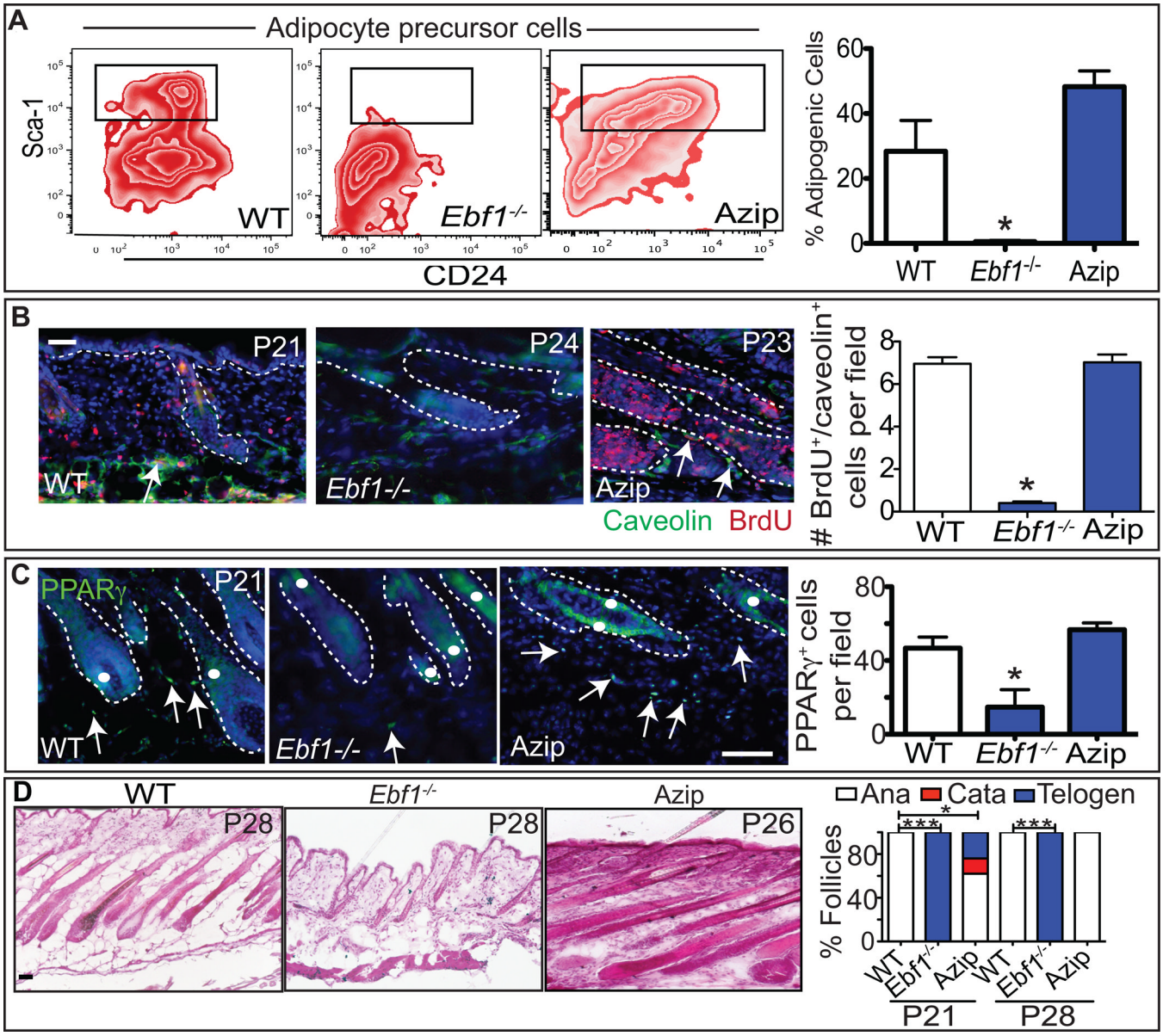

Figure 3. Defects in the generation of immature adipocyte lineage cells blocks follicle stem cell activation

A. FACS analysis of Sca1$^+$ adipogenic cells derived from WT, *Ebf1*$^{-/-}$ and Azip skin reveals an absence of adipocyte precursor cells in *Ebf1*$^{-/-}$ mice. n=3 mice. B. Analysis of BrdU incorporation during a 3-day pulse in caveolin$^+$ cells in the skin of WT, *Ebf1*$^{-/-}$ and Azip mice after P21. Arrows indicate BrdU$^+$ (red), caveolin$^+$ (green) cells within the intradermal region of the skin. C. Analysis of PPARγ expression (green, arrows) in the dermis of WT, *Ebf1*$^{-/-}$ and Azip mice. Dotted lines outline hair follicles. Dots indicate non-specific immunostaining. n=3 fields from 3 mice for each genotype. D. Analysis of anagen (Ana), catagen (Cata), and telogen hair stages in WT, *Ebf1*$^{-/-}$ and Azip mice based on morphology at indicated ages. n=5–7 mice; >37 follicles for each bar. All data are ± SEM, *p<0.05, *** p<0.0001. Bars=100μm. See also Figures S3 and S4.

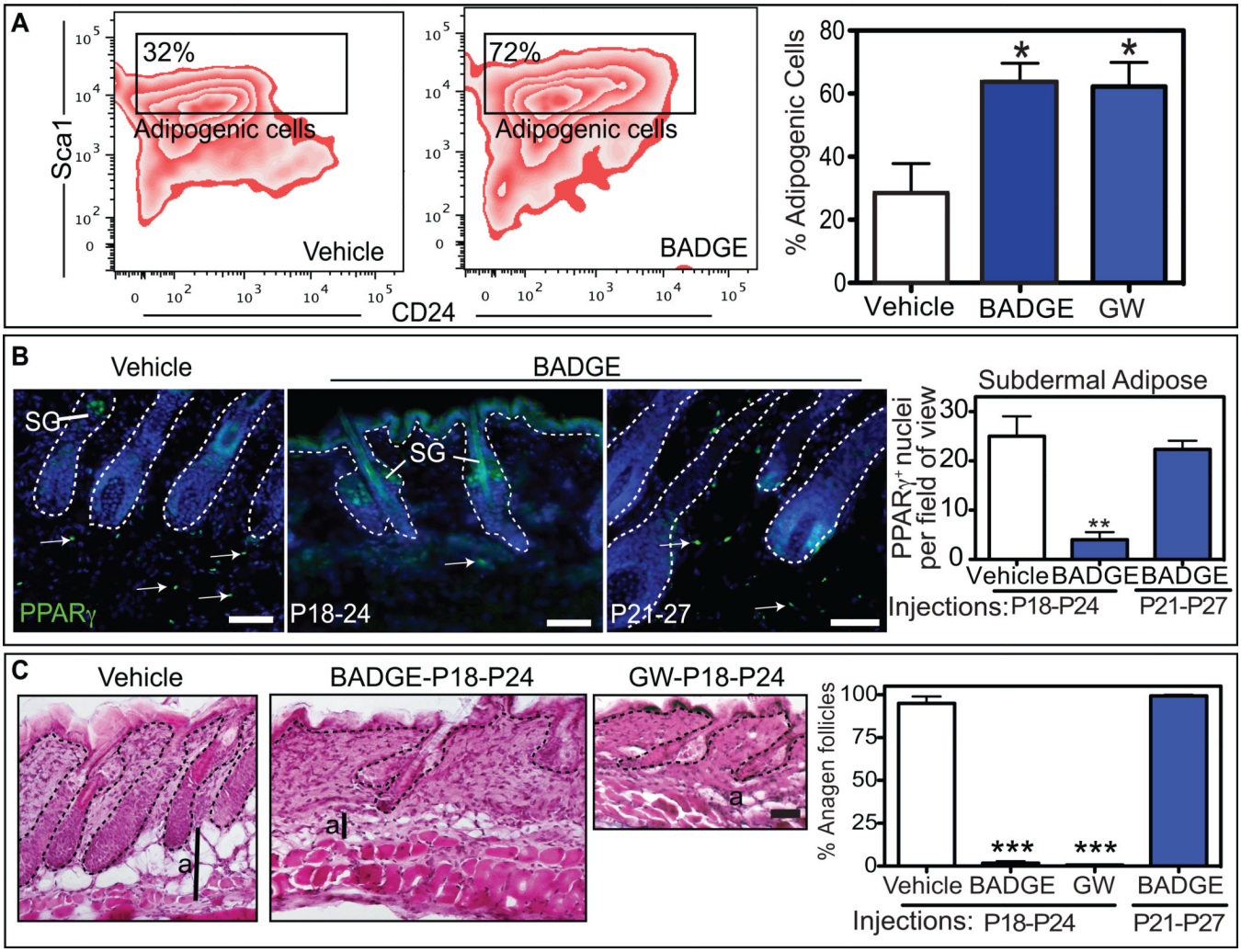

Figure 4. PPARγ antagonists abrogate intradermal adipogenesis and hair follicle stem cell activation

A. FACS analysis of Sca1$^+$ adipogenic cells derived from skin shows increased adipocyte precursor cells in BADGE and GW9662 (GW)-treated mice. n=3 mice. B. PPARγ immunostaining in vehicle and mice treated with BADGE either P18–P24 or P21–27. Arrows indicate PPARγ$^+$ cells. SG, sebaceous gland. n=3 mice; 3 fields of view. C. Analysis of anagen induction in mice injected with vehicle, BADGE, or GW for 6 days at indicated ages. All data are ± SEM, *p<0.05, **p<0.005, ***p<0.0005. Bars=100μm. See also Figure S5.

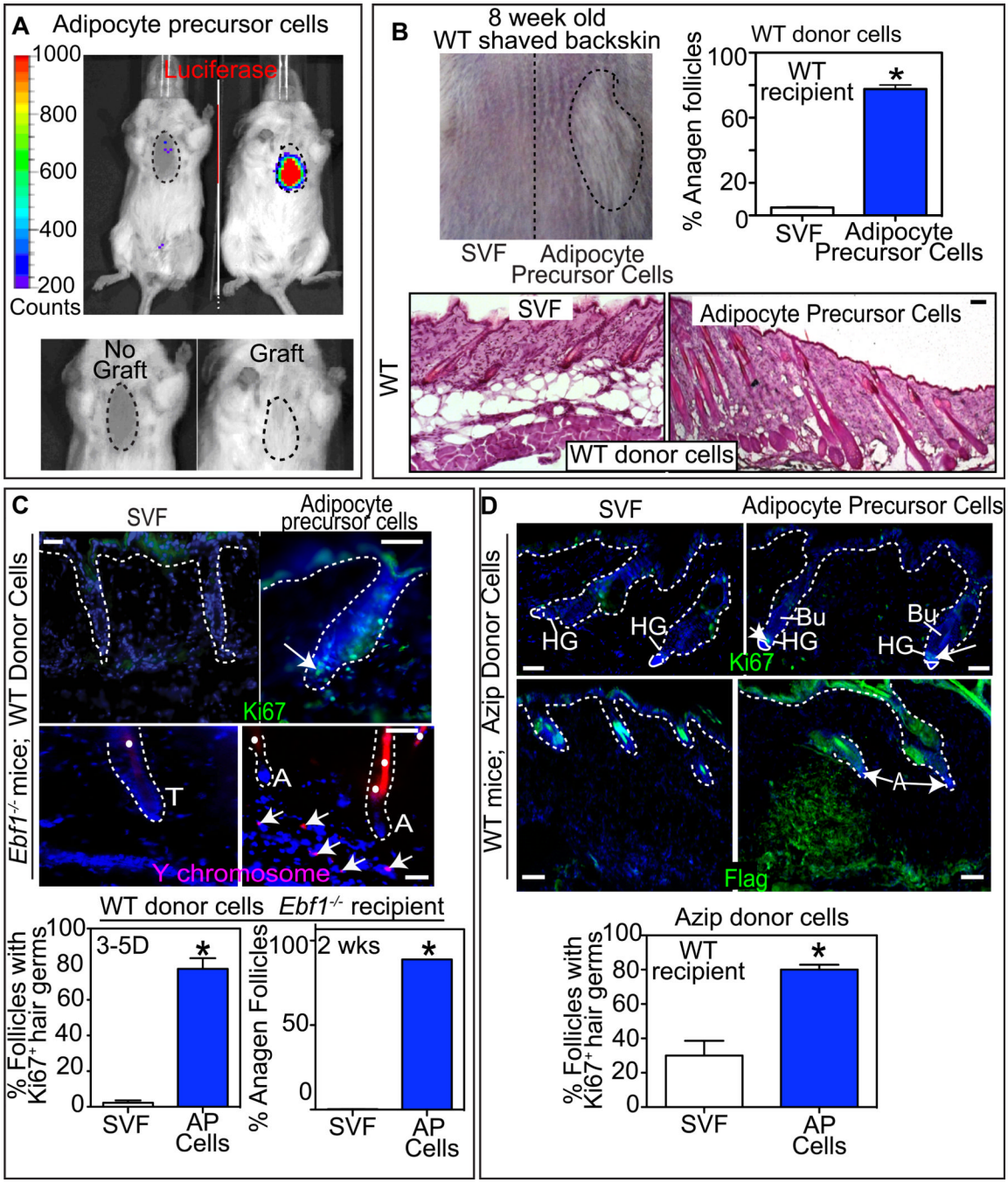

Figure 5. Adipogenic cells are sufficient to induce hair follicle regeneration

Analysis of anagen induction in mice injected with 50,000 stromal vascular fraction cells (SVF) or Sca1^{+} adipocyte precursor cells from indicated genotypes. A. Luciferase imaging of adipocyte differentiation 6 weeks after injection of adipocyte precursor cells derived from subcutaneous adipose tissue of FVB *leptin*-luciferase mice into shaved, 7-week old FVB WT recipient mice. B. After two weeks, WT adipocyte precursor cells induce hair growth when injected intradermally into shaved 8 week old backskin. Graph indicates quantification of anagen induction based on morphology of 35 follicles from 2 independent experiments. Histology of hematoxylin and eosin staining follicles from SVF or adipocyte precursor injected skin regions is shown. C. Intradermal injection of WT adipocyte precursor cells

induces anagen as indicated by proliferation ($Ki67^+$ cells, arrow) within hair germs of P21 *Ebf1*$^{-/-}$ mice after 3–5 days (D) or full anagen after 2 weeks (wks). *In situ* hybridization on skin sections of injected tissue reveals Y chromosome localization (arrows) in female *Ebf1*$^{-/-}$ skin after intradermal injection with FACS isolated adipocyte progenitors derived from male WT skin. A, anagen follicle; T, telogen follicle; AP, adipocyte precursor. Dots indicate autofluorescence. n>35 follicles from 2 independent experiments. D. Adipocyte precursor cells derived from Azip skin induce anagen in WT P49 skin 3D after intradermal injection as indicated by $Ki67^+$ hair germ cells (arrows). Flag epitope immunostaining of transplanted skin reveals the localization of $Flag^+$ transplanted cells in skin injected with adipocyte precursors. Arrows indicate anagen induction as indicated by enlarged, hair germs and $Ki67^+$ staining. AP, adipocyte precursor. n>27 follicles from 2 independent experiments. All data are ± SEM, *p<0.05. Bars=100μm.

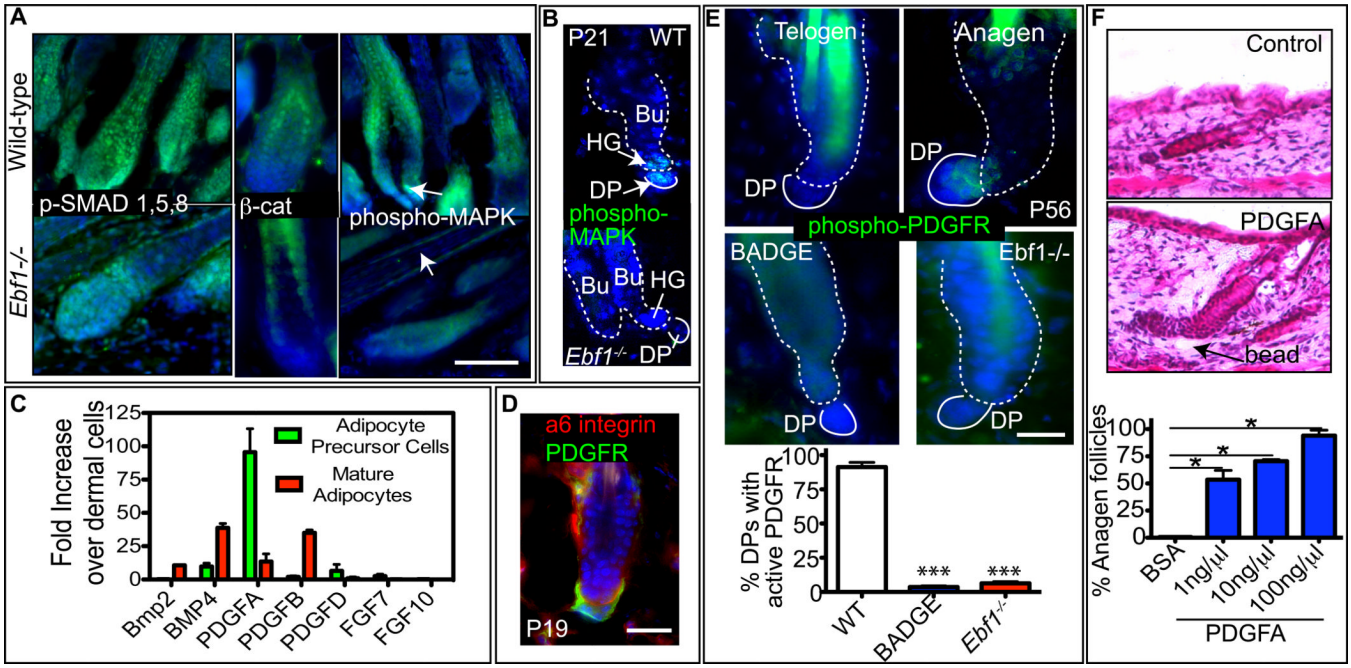

Figure 6. PDGF signaling in the skin requires intradermal adipocyte precursor cells

A. Immunostaining for phospho-SMAD(1, 5, 8), β-catenin, and phosphorylated p42/44 (MAP kinase) in skin sections of P7 WT and *Ebf1*$^{-/-}$ mice. Arrows indicate positive cells. B. Phospho-MAP kinase staining in vehicle and BADGE-treated mice at P24. Arrows indicate positive cells. Bu, bulge; HG, hair germ; DP, dermal papillae. C. Real-Time PCR analysis of mRNA expression in adipocyte precursor cells and mature intradermal fat compared to total isolated skin cells. n=3 independently isolated cell populations. D. PDGF receptor expression in telogen stage follicles (P19) localizes to the dermal papilla (DP) beneath the α6 integrin^{+} border with the hair follicle cells. E. Analysis of PDGF receptor activation in DP from WT (telogen (P49) and anagen (P56)), BADGE-treated (P24) and *Ebf1*$^{-/-}$ (P21) mice. Dashed lines mark the hair follicle, while solid lines mark the dermal papilla (DP). n=50–75 follicles in ≥2 mice for each sample. F. Hematoxylin and eosin stained follicles from *Ebf1*$^{-/-}$ mice injected with control or PDGF coated beads 5 days post-injection. Quantification of the dose response of anagen induction with beads coated with BSA or indicated concentrations of PDGFA. n=15–24 follicles from two independent experiments. All data are ± SEM, *p<0.05. ***p<0.001. Bars=100μm.

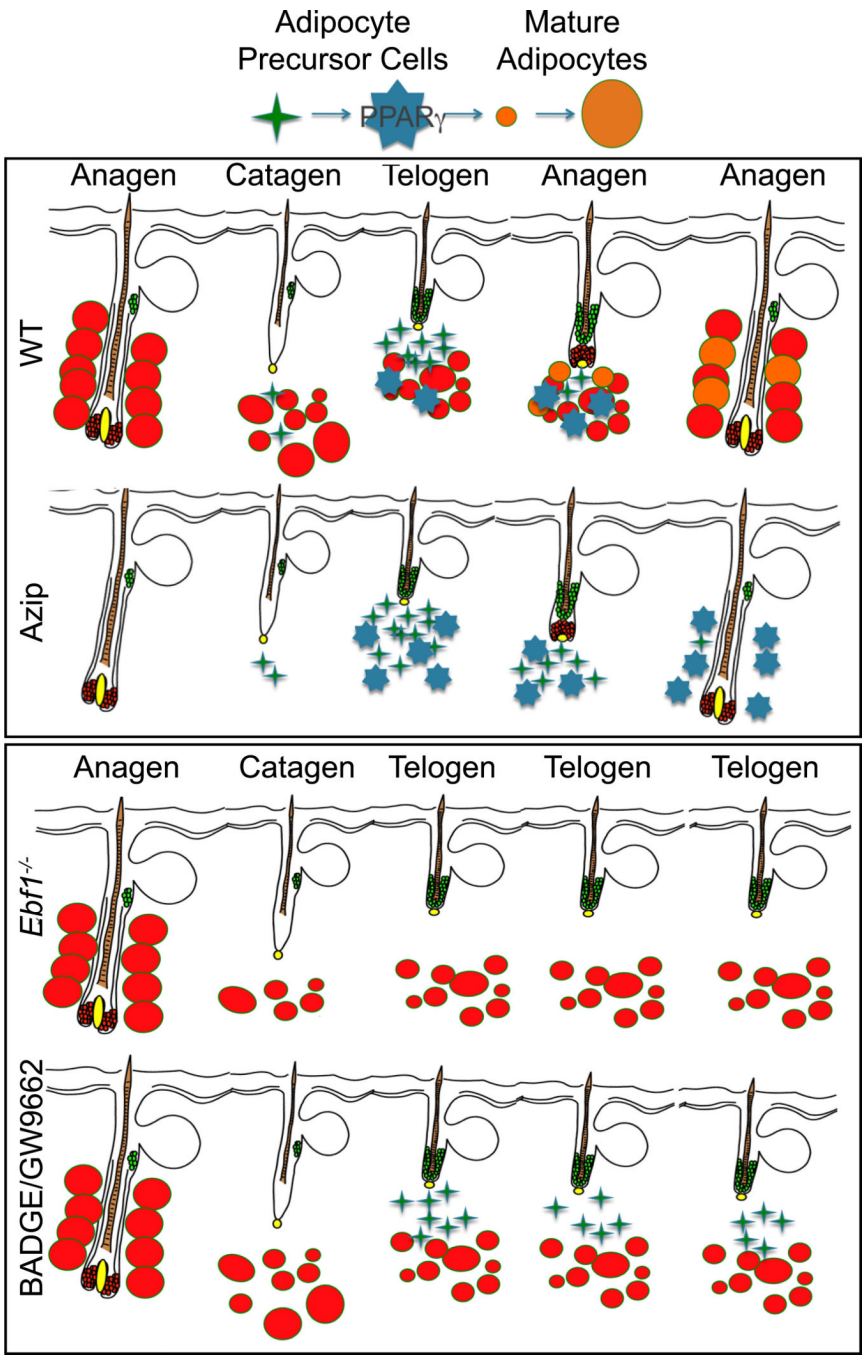

Figure 7. Model for the role of adipocytes in the skin in WT and mouse models with defects in adipogenesis

During the hair follicle cycle, intradermal adipose tissue increases size in part due to the activation of adipocyte precursor cells (green and blue stars) that generate new mature adipocytes (orange circles) *de novo*. Proliferation of adipocyte lineage cells is stimulated during follicle regression (catagen) to increase adipocyte precursor cell number during telogen and anagen initiation. Azip mice lack mature adipocytes but have adipocyte precursor cells and regenerate follicles similar to WT mice. In *Ebf1*$^{-/-}$ mice, adipocyte precursor cells are absent within the skin after catagen, leading to a reduction in intradermal adipose tissue and defects in stem cell activation. Similarly, treatment of mice with

PPARγantagonists during catagen blocks subdermal adipose tissue growth and follicle regeneration. However, the most immature adipocyte precursor cells are maintained in mice treated with PPARγ antagonists, suggesting that intradermal adipocyte precursor cells that express PPARγ(green star) are essential for sterm cell activation in the hair follicle.